



UWB MIMO antenna with hybrid pattern and polarization diversity

Original
Article

Abdallah S. Yousef¹, Ahmed M. Abdelraheem², Ashraf Mahran³, M.A. Abdalla⁴

Departments of ^{1,3}Avionics Engineering, ^{2,4}Electronic Engineering, Military Technical College, Cairo, Egypt

Keywords:

ECC, MIMO, pattern diversity, polarization diversity, UWB.

Corresponding Author:

Abdallah S. Yousef, Department of Avionics Engineering, Military Technical College, Cairo, Egypt, **Email:** abdallah.s.yousef@ieee.org

Abstract

This study introduces a detailed design architecture and analysis of a modified half disc monopole Ultra-Wideband (UWB) (3.110.6- GHz) antenna element used to build a multiple-input multiple-output MIMO with extra hybrid polarization and radiation pattern diversity. Three MIMO configurations demonstrated with full measurements for the scattering parameters and far-field antenna pattern are studied. A detailed comparative study was introduced between three different MIMO configurations to illustrate the effect of hybrid diversity techniques on MIMO performance. Analytical calculations performed to estimate various parameters such as Envelope Correlation Coefficient (ECC), Diversity Gain (DG), Total Active Reflection Coefficient (TARC), and channel gain matrix is deduced to fully describe the antenna system channel capacity performance in a full duplex telecommunication system. The MIMO parameters were obtained using both the scattering parameters and the farfield results. The enhancement in the MIMO performance comes along with the appropriate size of the antenna and improves the mutual coupling between MIMO elements.

1. INTRODUCTION

Wireless communication technology became a serious challenge among telecommunications giant developers. Various techniques are deeply investigated to reach millions of users' satisfaction, high Signal-to-Noise Ratio (SNR), moderate cost systems, high rate of data, heavy traffic channels, and the increasing number of users in modern systems^[1]. Also, human needs to control remotely their properties require multi-wireless connections for the same end-user profile. Ultra-wideband antennas have become a solution to overcome the problem of scarce bandwidth resources providing the most achievable channel capacity and higher data rates compared to single-band antennas^[2]. The Federal Communication Commission (FCC) regulated the Ultra-wideBand (UWB) from 3.1 to 10.6 GHz^[3] and licensed for short-range wireless communication applications such as high-speed LAN/WAN (+20Mbps), since the ultra-wideband antennas' typical applications are imaging through high data rate wireless applications and avoidance Rader, geolocation causing increasing demand on such antennas. UWB antennas give data rates greater than 100 Mbps using low power transmission levels^[4]. A low transmission power profile put UWB antennas at the top listed highly usage antennas in most commercial wireless systems especially for LANs/WANs, due to

their robustness for multi-path fading and low power dissipation. Many silicon manufacturers have developed solutions to UWB systems that allow it to coexist with other technologies however, there are many challenges for the UWB technology to reach an end. Mutual coupling is considered a key parameter, and the reduction of this parameter is a challenging purpose for RF researchers, It enhances spectrum efficiency, channel capacity, and communication reliability^[5]. Various techniques are used to overcome the problem of high average mutual coupling between MIMO elements such as etching uniform/non-uniform structures by making design changes in the ground plane known as defected ground structure. This technique is used in^[6] by inserting circuits to reduce the coupling^[7,8]. As a result of decreasing coupling, an acceptable level of correlation between antenna elements^[9] is reached. To make a MIMO operates with acceptable performance and enlarge the data rate while maintaining a maximum level of signal-to-noise ratio (SNR), the Envelope Correlation Coefficient (ECC) value should be less than 0.02 among the MIMO elements to ensure a better system acting in a communication link^[10].

MIMO antenna systems recently capture almost 37% telecommunication market by 2023^[11]. MIMO systems in collaboration with UWB technology fostered the existence of various solutions for these challenges offering

a better performance for MIMO systems by mixing both technologies^[12]. It treats almost every transmitter to receiver element as a standalone full duplex channel^[12,13], and It also allows the antenna to use certain codes for transmitting the data signal using a parallel simultaneous transmission. Reducing transmitting time and power level needed for transmission process utilizing low-cost telecommunications systems. In this case, the data rate equals multiple of the data rates obtained by using the single antenna (SISO) to get the MIMO channel gain matrix and then, obtain its channel capacity^[4].

The wireless communication channels suffer several impairments such as thermal noise, signal power path loss, and shadowing. A solution for the problem is to increase signal power while adding fading margin at the transmitter, however, the diversity concept validates a more efficient solution for fading problem^[12]. The diversity idea is to make several duplicates of the desired signal to give the recipient a chance to accumulate more power from the received signal providing a high-performance communication system^[14]. Diversity approaches are frequency diversity, Wireless link as MIMO offer a recipient (N) number of sights, These techniques are employed to combat both time and frequency fading^[15,16].

This paper introduce planar antenna structure cover the UWB with optimized design parameters, optimization process done through modifications in the ground plane to enhance the antenna reflection coefficient all over the entire wideband $S_{11} \leq -10$ dB as in section[II], antenna ground is simply reduced at the edges to have a good matching over the UWB. In section[III], MIMO theoretical brief is mentioned. In section[IV], design is developed from the single antenna until reaching three different (2x2) MIMO configurations, the design modifications performed on the elements position, enhanced ground plane and the mixed design is presented. In Section[V], the performance

of each configuration is simulated and measured. then, calculating MIMO S- parameters and far-field pattern components for post-processing output ECC, DG, TARC, and Channel Capacity Loss (CCL) in order to compare the results from S-paramerts and farfield compoents, presenting more accurate results. Then, according to these comaprison a better estimation what of the mentioned MIMO configurations is suitable for the intended type of communication link.

II. SINGLE ELEMENT CONSTRUCTION

The concept of UWB antenna design is to have a simple geometry with almost constant parameters over quite wide bandwidth^[17-19]. The proposed antenna is an optimized structure consisting of a ground plane and half circular radiator as shown in Fig. 1. The geometry contributes to the small size of $w_s \times l_s$ (40x40 mm), with planar structure printed over RO4350 substrate its thickness 1.52 mm. The single element is designed based on the best matched characteristic for the current on the skin of the radiator to get almost an Omnidirectional pattern over the range of UWB. The selection process of the antenna design parameters completely satisfies the design equations in^[19,20]. A rounded edges are used in the ground to reduce reflections, get higher performance, and hold a good matching in the desired band. The antenna element is fabricated as illustrated in Fig. 2, and The dimensions are $R = 14$ mm, $W_s = 40$ mm, $L_s = 40$ mm, $L_f = 19.7$ mm, $L_g = 19.5$ mm. through chamfering the edges of the antenna radiator also rounded edges are utilized for the ground.

The planar element had been simulated and its parameters is deduced at the UWB range. As shown in Fig. 3, the simulated and measured reflection coefficient is less than -10 dB within the frequency range from 3 GHz to 11 GHz which fairly agrees with the UWB spectrum.

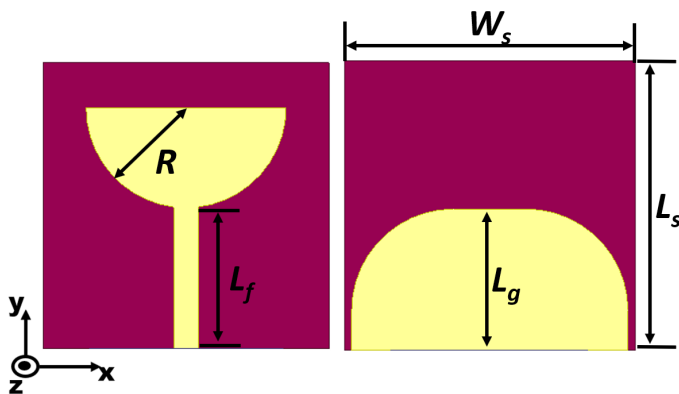


Fig. 1: Geometry of the planar microstrip UWB antenna



Fig. 2: Manufactured single-element antenna

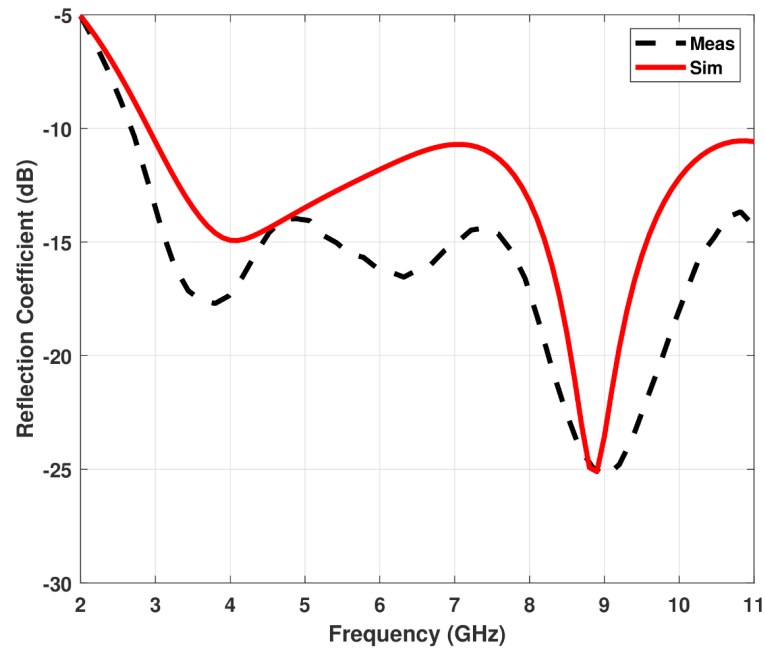


Fig. 3: Measured and simulated S11 for single-element antenna

Alamouti scheme was developed in 1988^[21]. MIMO channel can be modeled as:

$$\vec{Y} = \vec{H}\vec{X} + \vec{N} \quad (1)$$

Lately, MIMO-based systems use UWB radiators to provide higher multiplexing gain, increase the capacity of data links to handle the increased demand for higher data rates^[18,22], while keeping eyes on maintaining good MIMO performance over the wide band. This topic has been proposed in^[23-27]. In^[23], two crossed L-shape strips/stubs have been proposed to obtain MIMO antenna in UWB by using a slot in the antenna ground for reducing the mutual coupling. This approach increases the antenna performance at the (2.1–5.3) GHz band and at the (8.1–10.3) GHz band, however, the reflection coefficient in the (3.1–5.7) GHz band had become less than desirable. In^[25], the UWB configuration of BI triangle-shaped radiators with a shared ground has in the frequency portion (2.9–4.1) GHz and (6.1-8.9) GHz with an average between 9 - 20 dB isolation. Other techniques are decoupled by the cross-orientation for antennas^[26], by the use of perpendicular orientated MIMO elements, and add a slot between the elements^[24,27].

Diversity is used to enhance MIMO performance in high fading channels^[15,28-30]. The alternative solution of transmitting and receiving the intended data through a single channel is to obtain an M replica of the intended data

Where \vec{X} represents the transmitted signal by Nr antennas, \vec{N} represents the noise vector, \vec{Y} represents the received signal, and \vec{H} represents the path gain along the channel between transmitter and receiver antennas.

through N channels, While some copies may suffer fades, others may not, still, the receiver obtains energy enough to make the right decision on the received data symbol. Different techniques of diversity are commonly employed in wireless communication systems.

III. BUILDING MIMO CONFIGURATION

In this section, a constructed MIMO configuration based on a single element antenna demonstrated in section (II) is introduced. The diversity concept is implemented through achieving the techniques of polarization diversity by MIMO antenna perpendicular elements and pattern diversity by controlling the power fed to each port of the antenna at all MIMO configurations. Also, a reduced ground structure improved the coupling between the elements by a value of less than -20 dB, so it could enhance the MIMO system's reliability^[24]. Moreover, the antenna elements are maintaining the reflection coefficient of the MIMO below ≤ -10 dB to provide good matching all the frequency range.

MIMO first configuration is built by adding two constitutive elements of the proposed antenna element

while the edge-to-edge distance is less than 0.2λ as shown in Fig. 4. a named without diversity full ground (WO-FG) and Fig. 5.a for the fabricated prototype. The configuration is modified by means of diversity in pattern to enhance the MIMO performance and achieve an almost isotropic pattern in both vertical and horizontal components as shown in Fig. 4.b named with diversity full ground (W-FG) and Fig. 5.b for the fabricated prototype. Further modifications are added to the antenna ground to reduce the mutual coupling between the two antennas as in Fig. 4.c named with diversity reduced ground

(W-RG) and Fig. 5.c for the fabricated prototype; all in the same substrate, good antenna matching S_{11} , S_{22} as well as lower mutual coupling S_{12} , S_{21} as in Fig. 6 and Fig. 7. The measured and simulated radiation patterns for all MIMO configurations in both planes XZ, and YZ at selected frequencies (5 GHz, 7 GHz, and 9 GHz had been illustrated in Fig. 8, Fig. 9, and Fig. 10, respectively, these figures are illustrating the normalized pattern in both axis mentioned, for further illustration about the levels of cross polarization the 3D total gain is illustrated in Fig. 11 which contributes to low levels of cross polarization.

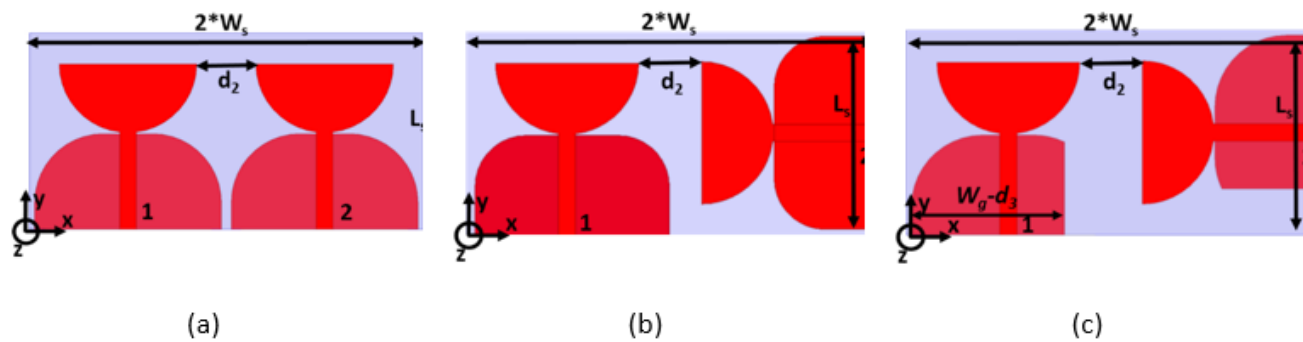


Fig. 4: UWB MIMO antenna configurations (a)WO-FG, (b)W-FG, (c)W-RG

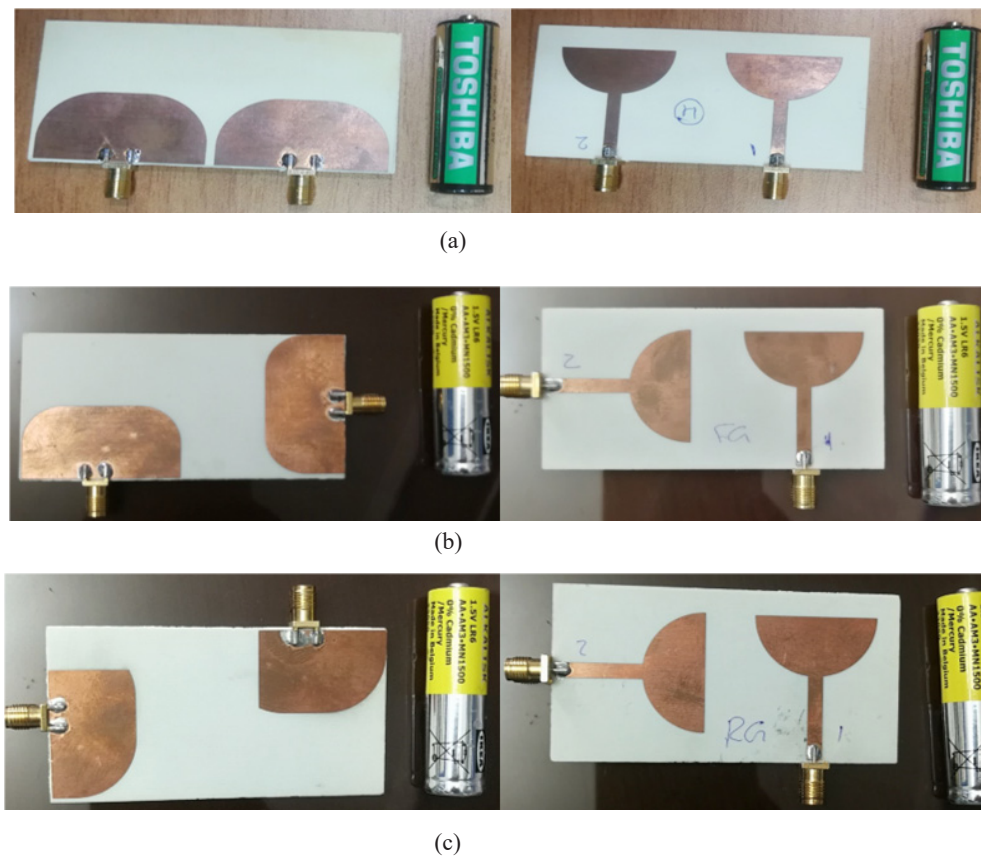


Fig. 5: Manufactured UWB MIMO antenna configurations (a)WO-FG, (b)W-FG, (c)W-RG

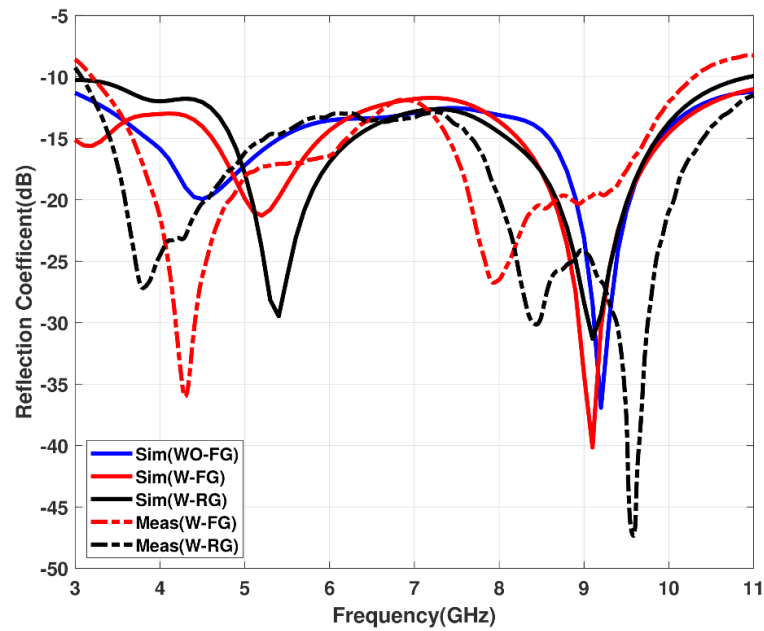


Fig. 6: Reflection Coefficient for MIMO configurations

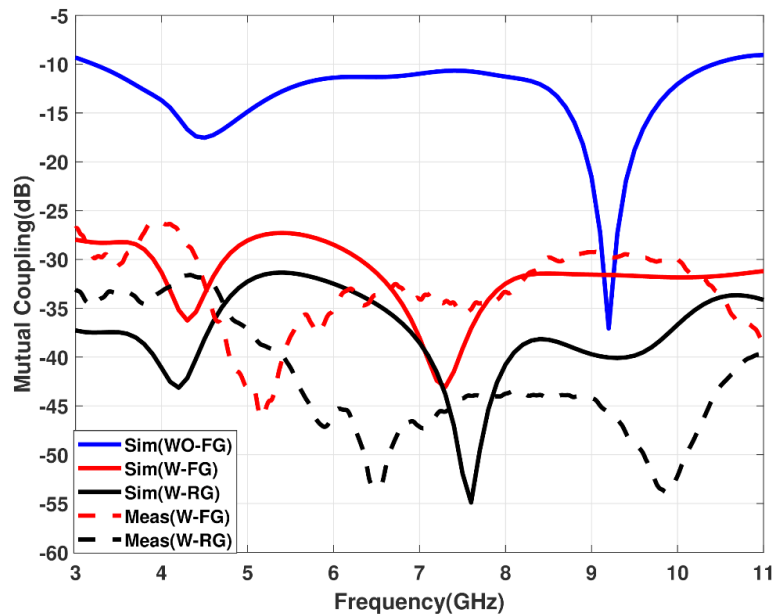


Fig. 7: Mutual coupling for MIMO configurations

In figure 6, the reflection coefficient of MIMO configurations are illustrated to show that all lies below -10 dB. while in figure 7, the mutual coupling between elements is shown for (WO- FG) it have high

correlation, this problem is solved by (W-FG) to have average correlation of -30 dB, and then optimized by (W-RG) to reach an average value of -40 dB with -10 dB enhancement level.

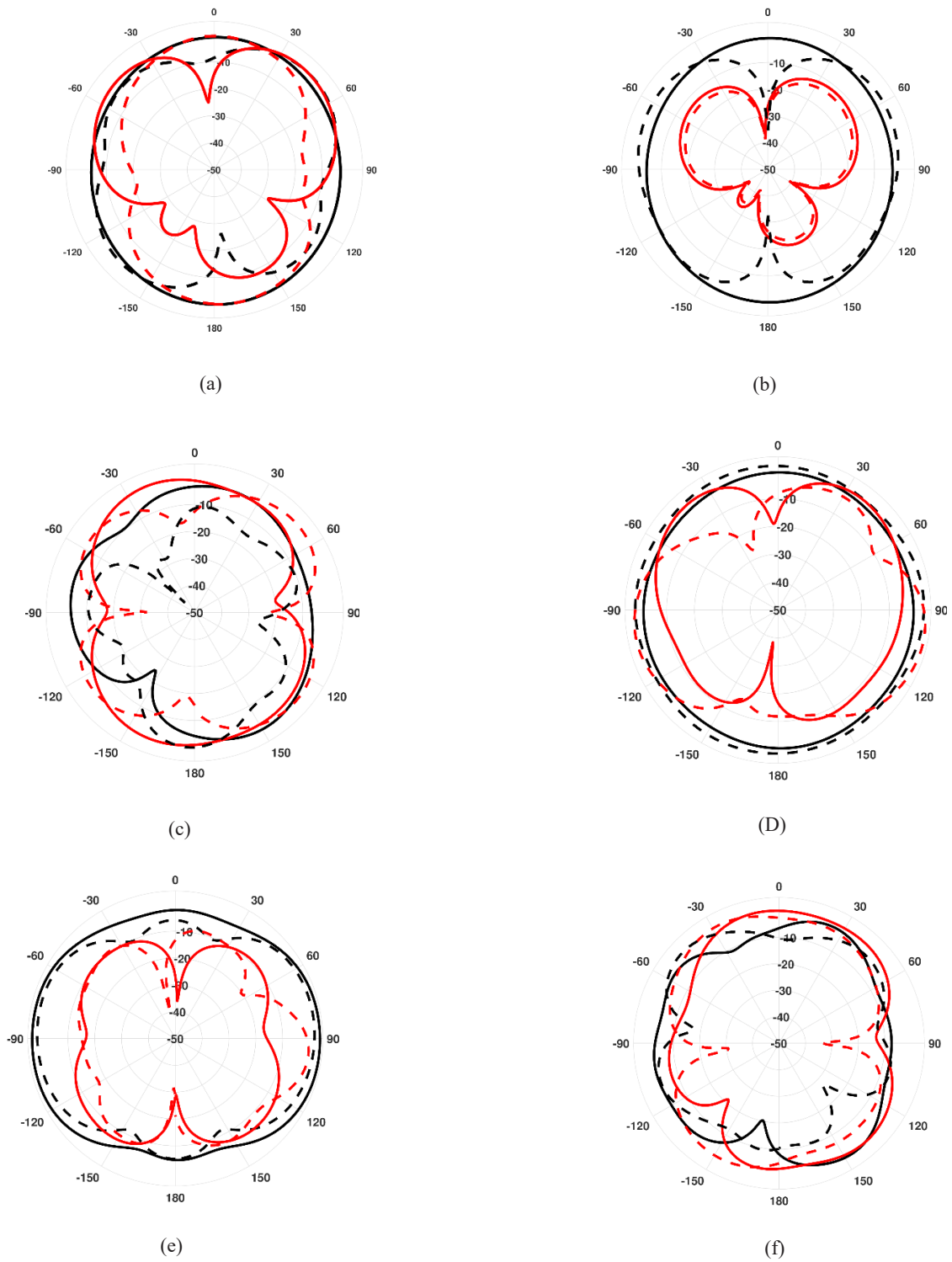


Fig. 8: Simulated and Measured radiation patterns for MIMO configuration in fig.4.a (a) xz-plane at 5GHz (b) xy-plane at 5GHz (c) xz-plane at 7GHz9GHz (d) xy-plane at 7GHz (e) xz-plane at (f) xy-plane at 9GHz

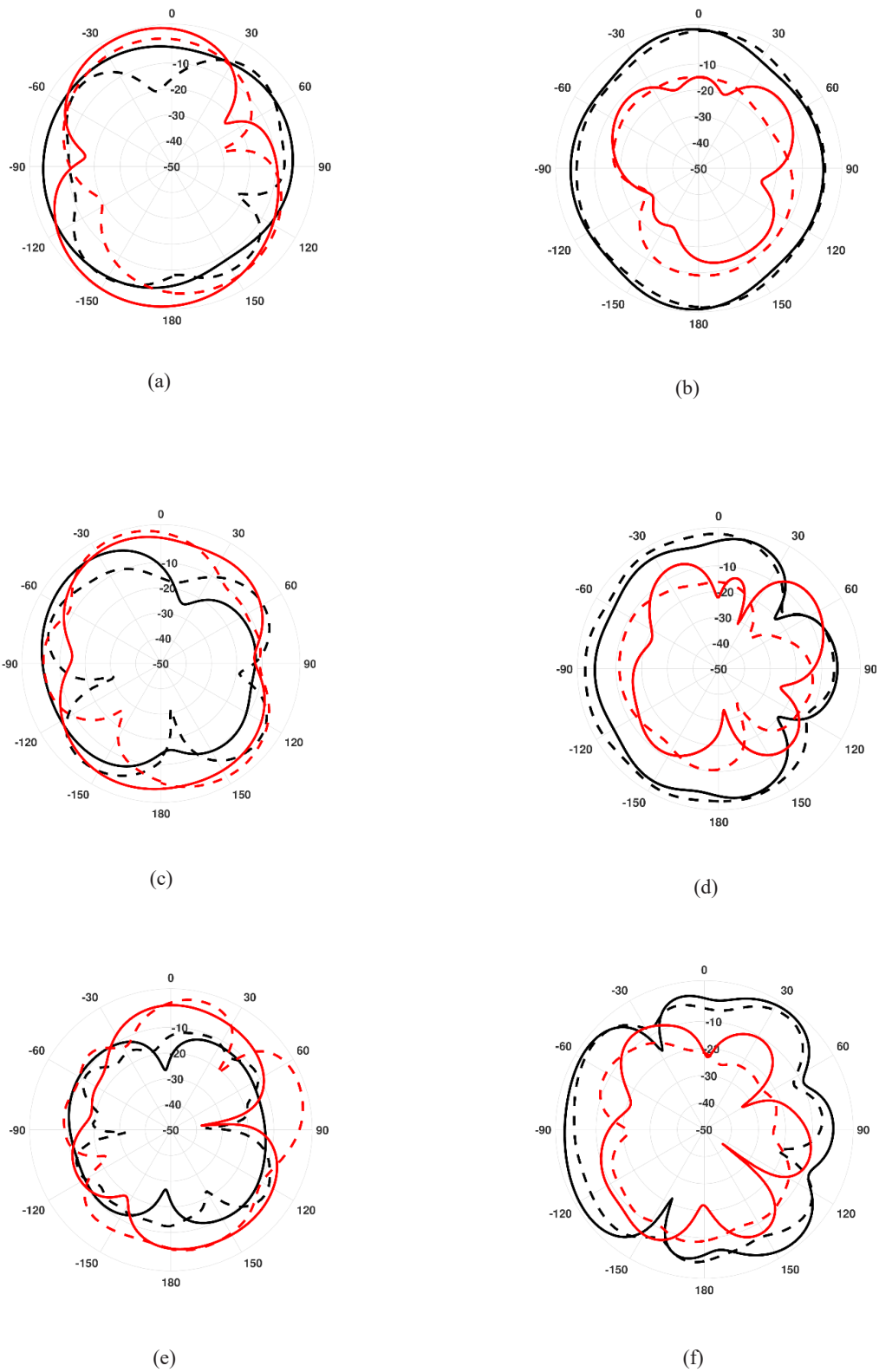


Fig. 9: Simulated and Measured radiation patterns for MIMO configuration in fig.4.b (a) xz-plane at 5GHz (b) xy-plane at 5GHz (d) xy-plane at 7GHz (c) xz-plane at 7GHz (e) xz-plane at 9GHz (f) xy-plane at 9GHz

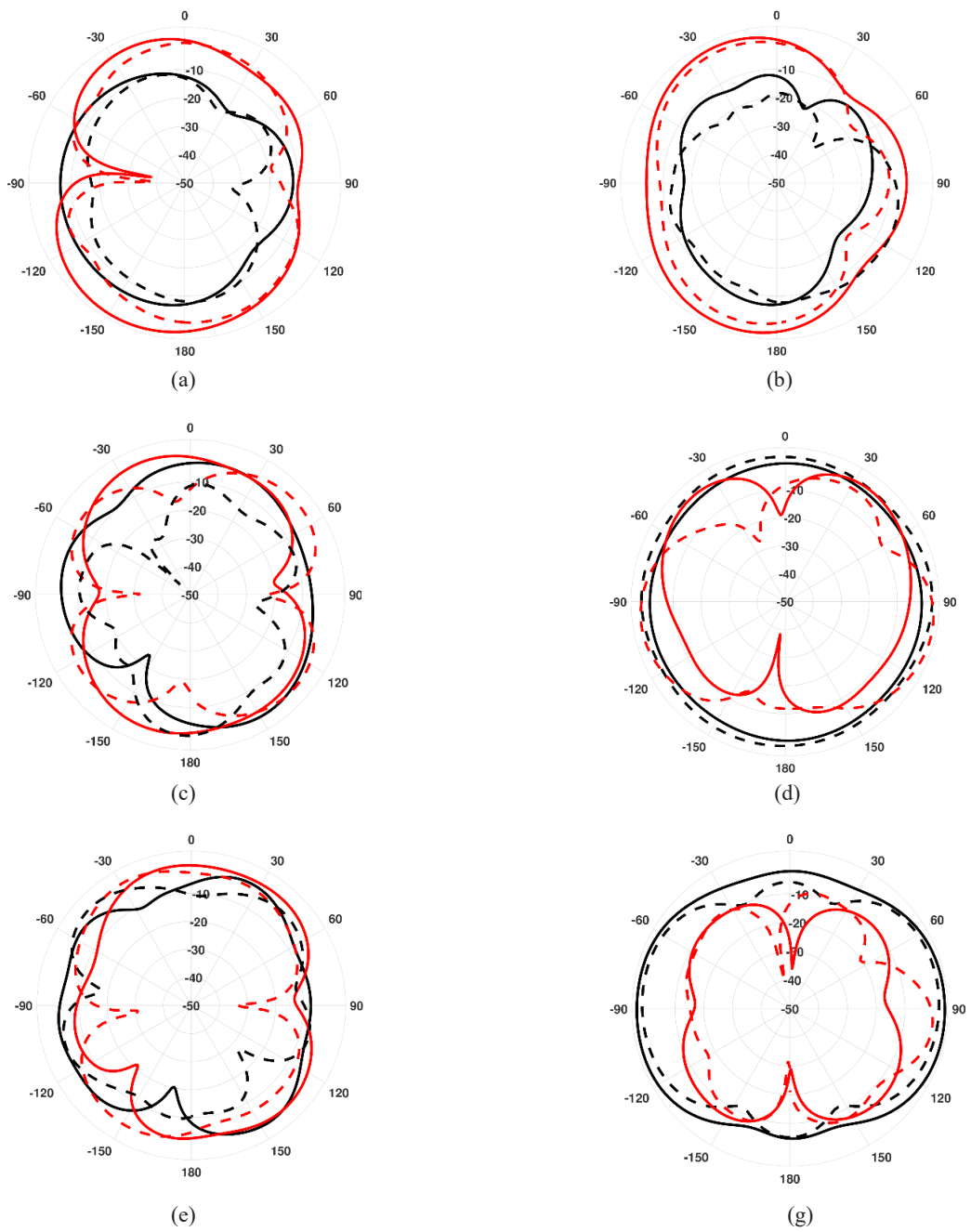


Fig. 10: Simulated and Measured radiation patterns for MIMO configuration in fig.4.c (a) xz-plane at 5GHz (b) xy-plane at 5GHz (c) xz-plane at 7GHz (d) xy-plane at 7GHz (e) xz-plane at 9GHz (f) xy-plane at 9GHz

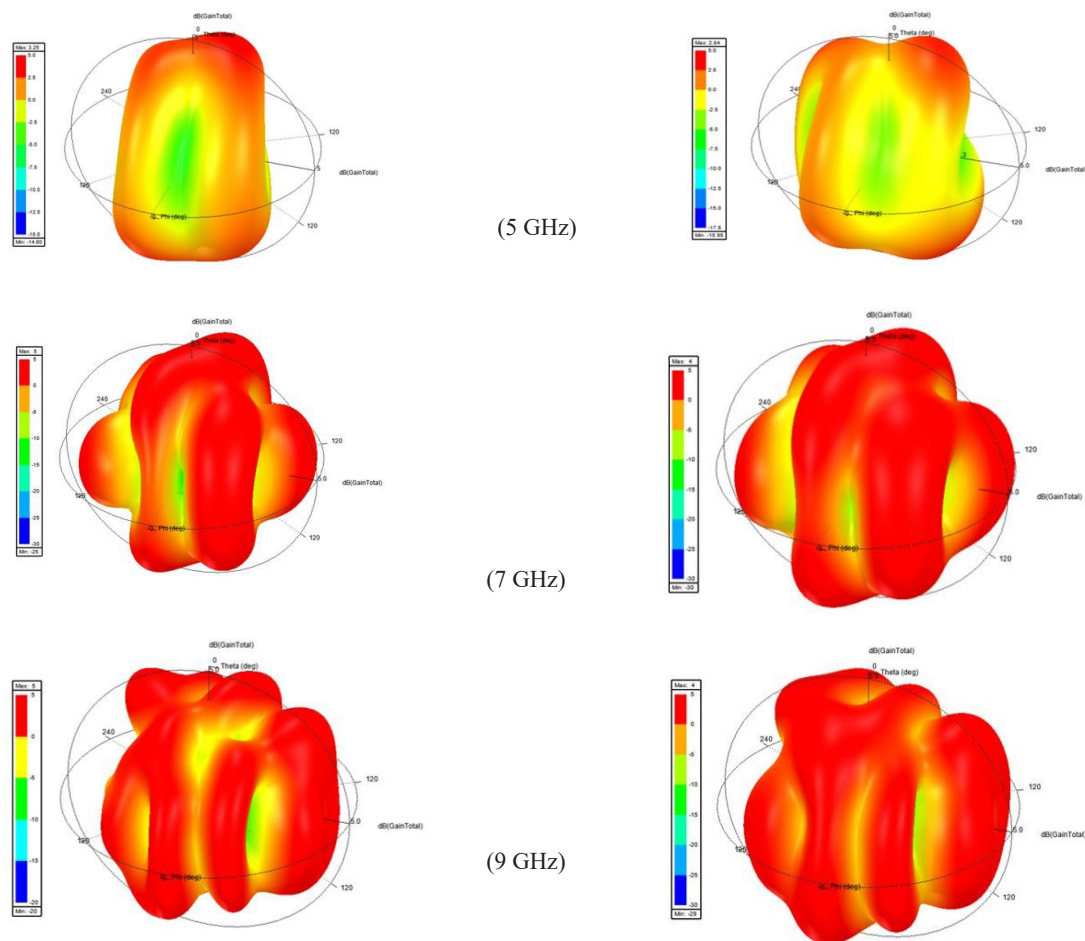


Fig. 11: total gain 3d (a)W-FG, (b)W-RG

In figure 11, total 3D gain for (W-FG) and (W-RG) are illustrated at snaps of the frequency band to show that the MIMO configurations is optimized to have good performance without affecting the shape of gain pattern, also to make it clear about the cross polarization for the designed MIMO.

IV. MIMO PERFORMANCE EVALUATION

In this section, further demonstrations are conducted for the MIMO antenna performance and the system has been evaluated by calculating envelope correlation coefficient (ECC)^[35,36], diversity gain (DG), and channel capacity loss (CCL) for each configuration, These parameters are vital to have a high-capacity uncorrelated channel, also the DG is a cornerstone parameter for MIMO system evaluation, CCL is used to measure the performance of MIMO system, it increases linearly according to the number of the MIMO system antenna elements^[37]. A further processing is calculated for three MIMO configurations and comparative illustrations are discussed in this section.

ECC is evaluated through two approaches, the first well known approach using the MIMO antenna scattering parameters as in Eqn (2) to get the ECC, this approach is used with sufficient accurate results for highly efficient antennas.

$$ECC = \frac{|S_{11}^* S_{12} + S_{21}^* S_{22}|^2}{(1 - (|S_{11}|^2 + |S_{21}|^2))(1 - (|S_{22}|^2 + |S_{12}|^2))} \quad (2)$$

The second approach is used in case of the antenna system is not highly efficient. Also, the antenna radiation pattern had been not accounted in the first approach. Therefore, another formula in (3) is conducted to calculate ECC considering the radiation patterns. the calculations of ECC by this approach are complicated as well. The measurement setup of MIMO configurations are precisely done to have an accurate result.

$$ECC = \frac{\left| \int_{4\pi} F_i(\theta, \phi) F_j^*(\theta, \phi) d\Omega \right|^2}{\int_{4\pi} |F_i(\theta, \phi)|^2 d\Omega \int_{4\pi} |F_j(\theta, \phi)|^2 d\Omega} \quad (3)$$

ECC accepted range is below 0.05^[37]. ECC of the proposed MIMO antenna is shown in Fig. 11, using formula (2), and the ECC conducted in Fig. 12, using formula (3). Hybrid diversity along the three configured combinations of the MIMO antenna system. Also, DG is derived using formula (4), Illustrated in Fig. 11, and Fig. 12 upon the scattering parameters and far-field formulas, respectively.

MIMO parameters are calculated by the two formulas

mentioned in eqns. (2) and (3), the ECC calculated from the S parameters formula in Eqn (2) is below 0.02 for the entire band which indicates stability in the performance of the MIMO antenna system, also the diversity gain derived from the formula in Eqn (4). Further calculations are performed for the ECC by using its far-field pattern based on the formula (3) to enhance the accuracy of the result as illustrated in Fig. 12, it can be noticed that its higher values than values derived from the S-parameters, however, still <0.02.

MIMO configurations simulated and measured reflection coefficient is illustrated in Fig. 6 it is shown the difference in the response for each configuration. In configuration one, the two radiators are allocated side by side without any modifications to the ground structure mentioned as (WO-FG). In configuration two, each antenna element is orthogonal to each other so its radiation patterns achieve the diversity desired from the design mentioned as (W-FG). In the last configuration the antenna radiators are the same like in (W-FG) but the ground structure for each element is modified to decrease the mutual coupling between the antennas to enhance the overall MIMO performance in the channel and this configuration is mentioned as (W-RG), these configurations reflection

coefficient satisfy the antenna design rules less than -10 dB all over the frequency band. The Mutual coupling between the antennas in (WO-FG) is -15 dB on average over the band. For (W-FG) the mutual coupling reaches -35 dB on average by almost -20 dB enhancement level and optimized in (W-RG) to become -40 dB in average. The simulated and measured results are illustrated for the MIMO configurations in Fig. (7).

The ECC is evaluated by formula 2,3 and the difference between the results is illustrated in Fig. 12, 13 and Fig. 14 for simulated and measured ECC derived from S-parameters respectively. Also, DG presented by Eqn (4) is used to appraise the MIMO system mentioned in Fig. 12, Fig. 13 and Fig. 14 in association with ECC for the contributed MIMO configurations.

$$DG = 10\sqrt{10} (\rho)^2 \quad (4)$$

It is shown that the ECC values for the whole UWB MIMO antennas are below 0.02 while, for the MIMO antenna DG, it is almost 10 dB for the entire band.

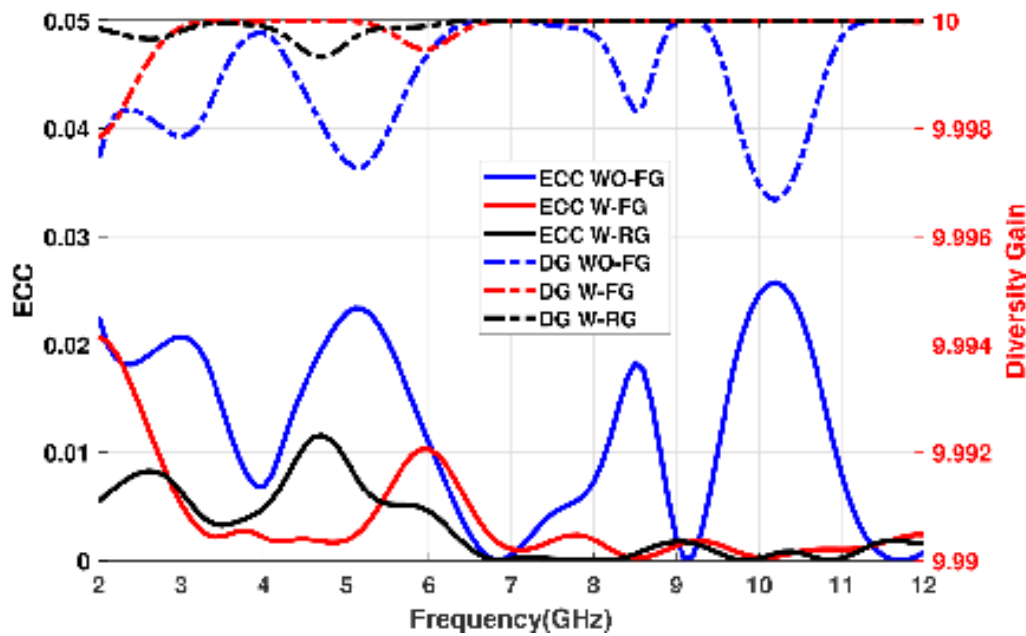


Fig. 12: Simulated envelope correlation coefficient and diversity gain for MIMO configurations derived from S parameters

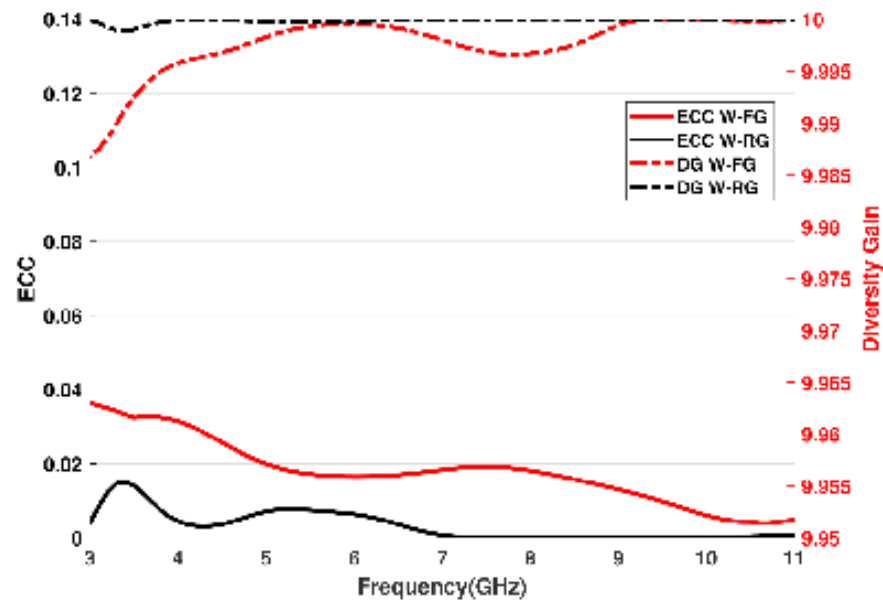


Fig. 13: Simulated envelope correlation coefficient and diversity gain for MIMO configurations derived from the far field- parameters

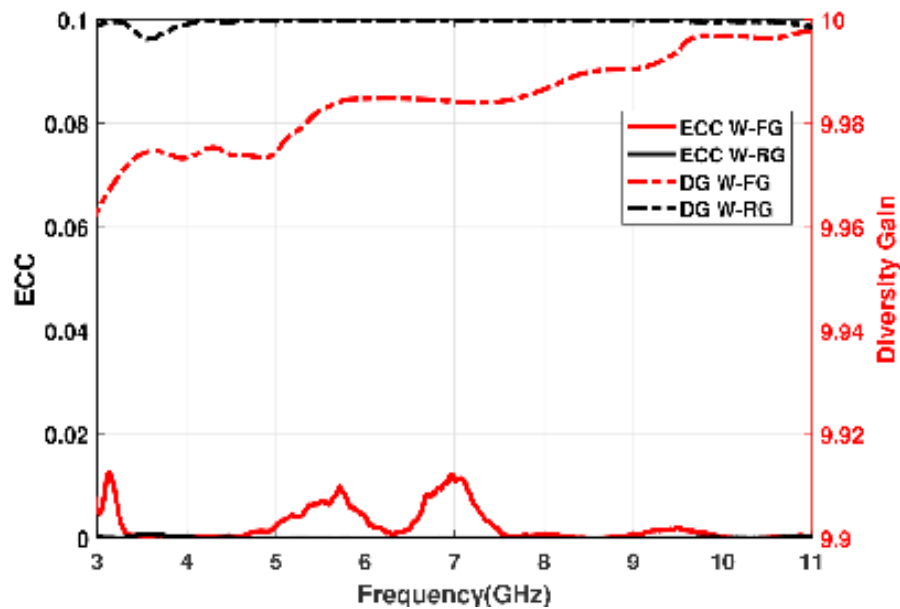


Fig. 14: Measured envelope correlation coefficient and diversity gain for MIMO configurations derived from S parameters

Finally, the MIMO TARC is illustrated in Fig. (15) show almost stable performance for the MIMO channels with enhanced TARC results in (W-RG) than that in (W-FG), led us to the CCL calculated as in equations 5, 6, 7 (a,b)^[38,39]. The CCL is calculated upon each

configuration results. The simulated and measured CCL is plotted in Fig. (16), which had a mean value equal to 0.2 bits/s/Hz lower than the reference value of 0.4 bits/s/Hz within the UWB bandwidth^[38].

$$CCL = -\log_2 \det(\psi^R) \quad (5)$$

$$\rho_{ii} = 1 - (|S_{ii}|^2 + |S_{ij}|^2) \quad (7a)$$

$$\psi^R = \begin{pmatrix} \rho_{11} & \rho_{12} \\ \rho_{21} & \rho_{22} \end{pmatrix} \quad (6)$$

$$\rho_{ij} = (S_{ii}^* S_{ij} + S_{ji}^* S_{ij}) \quad (7b)$$

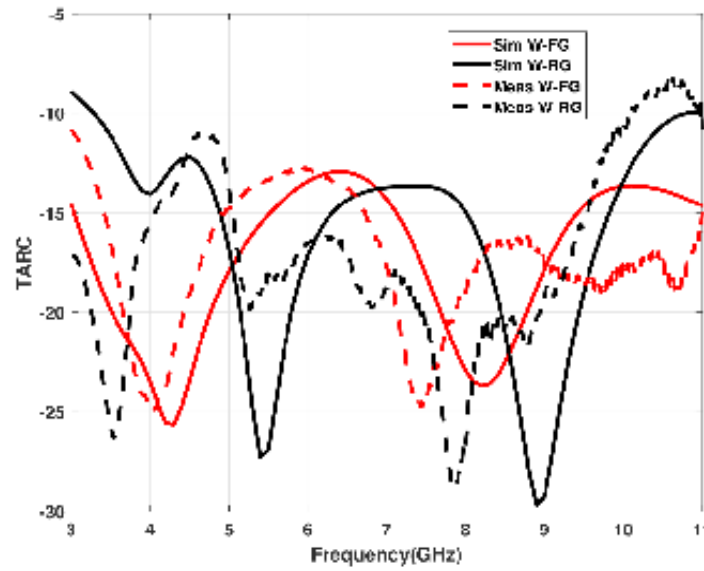


Fig. 15: Measured and Simulated TARC for antenna configuration

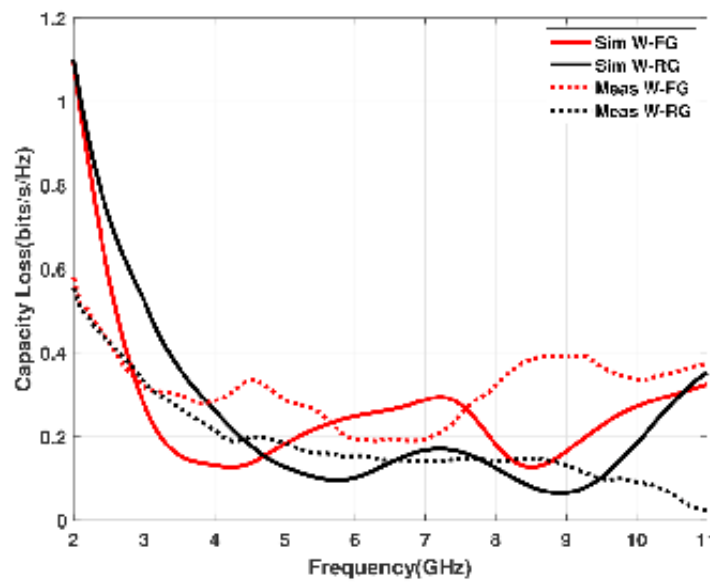


Fig. 16: The simulated and measured channel capacity loss of MIMO antennas.

**Table 1:** Comparison with recent work

Reference	Avg. Isolation	BW (%)	Technique
24	-12 dB	UWB (95 %)	I shaped slot
25	-20 dB	UWB (104 %)	Ground etching
26	-15 dB	UWB (120 %)	T-shaped stub
27	-5 dB	UWB (110 %)	Gnd slot
40	-12 dB	UWb (100 %)	Orthogonal orientation
41	-9 dB	UWB (101 %)	T shaped stub
42	-15 dB	UWB (100 %)	Decoupling vias
43	-12 dB	UWB (100 %)	Metallic strips
This work	-25 dB	UWB (134 %)	Cross orientation

V. CONCLUSION

A full MIMO antenna system architecture is introduced starting with a good candidate UWB single element with illustration for its properties measured and simulated all over the frequency band, a comparative study has been conducted based on this single element to form 3 different MIMO configurations each with its properties to serve different Telecommunications applications. All parameters are calculated for both simulated and measured data for the on-focus MIMO configuration. It is shown that it have a stable performance at UWB (3.1 GHz-10.6 GHz). MIMO configurations' radiation patterns are enhanced to reach almost Omni-directional pattern as proved in snaps at selected frequencies covering the entire band. High isolation is achieved through modifications in the ground structure of more the -35 dB on average to increase the MIMO diversity and enhance the performance of the signal in the channel to allow higher data rate and less channel capacity loss as illustrated at 0.2 b/s/Hz on average. The ECC parameter is also conducted from simulations and measurements for MIMO configurations beside derivations for the diversity gain. In addition, the antenna demonstrated typical MIMO parameters in terms of its ECC, DG, and channel capacity loss of less than 0.2 bits/s/Hz. Table of comparison with recent work is mentioned to make a clear vision about the contribution in this work.

VI. REFERENCES

- [1] A. L. Swindlehurst, E. Ayanoglu, P. Heydari, and F. Capolino, "Millimeter-wave massive MIMO: the next wireless revolution?" *IEEE Communications Magazine*, vol. 52, no. 9, pp. 56–62, 2014.
- [2] T. S. Rappaport, S. Sun, R. Mayzus, H. Zhao, Y. Azar, K. Wang, G. N. Wong, J. K. Schulz, M. Samimi, and F. Gutierrez, "Millimeter wave mobile communications for 5g cellular: It will work!" *IEEE Access*, vol. 1, pp. 335–349, 2013.
- [3] F. COMMUNICATION COMMISSION, "Revision of part 15 of the commission's rules regarding ultra-wide-band transmission system," *Tech. Rep.*, 02 2002.
- [4] B. Allen, M. Dohler, E. Okon, W. Malik, A. Brown, and D. Edwards, *Ultra-Wideband Antennas and Propagation: For Communications, Radar and Imaging*. John Wiley and Sons, 2006.
- [5] X. Chen, S. Zhang, and Q. Li, "A review of mutual coupling in mimo systems," *IEEE Access*, vol. 6, pp. 24 706–24 719, 2018.
- [6] Q. Li, M. Abdullah, and X. Chen, "Defected ground structure loaded with meandered lines for decoupling of dual-band antenna," *Journal of Electromagnetic Waves and Applications*, vol. 33, no. 13, pp. 1764–1775, 2019. [Online]. Available: <https://doi.org/10.1080/09205071.2019.1643261>.
- [7] M. Abdullah, Q. Li, W. Xue, G. Peng, Y. He, and X. Chen, "Isolation enhancement of Mimo antennas using shorting pins," *Journal of Electromagnetic Waves and Applications*, vol. 33, no.10, pp. 1249– 1263, 2019. [Online]. Available: <https://doi.org/10.1080/09205071.2019.1606738>.
- [8] X. Chen, M. Abdullah, Q. Li, J. Li, A. Zhang, and T. Svensson, "Characterizations of mutual coupling effects on switch-based phased array antennas for 5g millimeter-wave mobile communications," *IEEE Access*, vol. 7, pp. 31 376–31 384, 2019.
- [9] D. Wu, S. Cheung, T. Yuk, and L. Liu, "Design of a printed multiband Mimo antenna," in 2013 7th European Conference on Antennas and Propagation (EuCAP), 2013, pp. 2020–2023.
- [10] A. PAULRAJ, D. GORE, R. NABAR, and H. BOLCSKEI, "An overview of mimo communications - a key to gigabit wireless," *Proceedings of the IEEE*, vol. 92, no. 2, pp. 198–218, 2004.
- [11] M. R. Future®, "Massive MIMO market research report—global forecast till 2023," *Tech. Rep.*, 06 2020.
- [12] A. F. Molisch, *Wireless communications*. John Wiley and Sons, 2012, vol. 34.
- [13] W. Q. Malik and D. J. Edwards, "Measured mimo capacity and diversity gain with spatial and polar arrays in ultrawideband channels," *IEEE Transactions on Communications*, vol. 55, no. 12, pp. 2361–2370, 2007.
- [14] D. J. Love and R. W. Heath, "Limited feedback diversity techniques for correlated channels," *IEEE Transactions on Vehicular Technology*, vol. 55, no. 2, pp. 718–722, 2006.
- [15] K. Huang and Z. Wang, *Advanced Diversity Over Mimo Channels*, 2011, pp. 163–185.
- [16] A. M. Abdelraheem, A. Elsaieed, M. A. Abdalla, and A. Mahran, "Hybrid diversity for ECC enhancement of uwb Mimo antenna," in 2016 IEEE International Symposium on Antennas and Propagation (APSURSI). IEEE, 2016, pp. 1765–1766.
- [17] A. M. Abdelraheem and M. A. Abdalla, "Compact curved half circular disc-monopole uwb antenna," *International Journal of Microwave and Wireless Technologies*, vol. 8, no. 2, p. 283–290, 2016.
- [18] T. Kaiser, F. Zheng, and E. Dimitrov, "An overview of ultra-wide-band systems with MIMO," *Proceedings of the IEEE*, vol. 97, no. 2, pp. 285– 312, Feb 2009.
- [19] C. A. Balanis, *Antenna theory: analysis and design*. John Wiley and sons, 2016. [20] H. J. Visser, *Antenna theory and applications*. John Wiley and Sons, 2012.
- [21] S. Alamouti, "A simple transmit diversity technique for wireless communications," *IEEE Journal on Selected Areas in Communications*, vol. 16, no. 8, pp. 1451–1458, 1998.
- [22] A. Abdelraheem and M. Abdalla, "Bi-directional uwb Mimo antenna

- for superior spatial diversity, and/or multiplexing mimo performance,” *Wireless Personal Communications*, vol. 101, 08 2018.
- [23] J.-Y. Deng, L.-X. Guo, and X.-L. Liu, “An ultrawideband Mimo antenna with a high isolation,” *IEEE Antennas and Wireless Propagation Letters*, vol. 15, pp. 182–185, 2016.
- [24] J. Ren, W. Hu, Y. Yin, and R. Fan, “Compact printed Mimo antenna for uwb applications,” *IEEE Antennas and Wireless Propagation Letters*, vol. 13, pp. 1517–1520, 2014.
- [25] R. Kumar and G. Surushe, “Design of microstrip-fed printed uwb diversity antenna with tee crossed shaped structure,” *Engineering Science and Technology, an International Journal*, vol. 19, 01 2016.
- [26] S. Naser and N. Dib, “Design and analysis of super-formula-based uwb monopole antenna and its mimo configuration,” *Wireless Personal Communications*, vol. 94, 06 2017.
- [27] E. Yetisir, C.-C. Chen, and J. L. Volakis, “Low-profile uwb 2-port antenna with high isolation,” *IEEE Antennas and Wireless Propagation Letters*, vol. 13, pp. 55–58, 2014.
- [28] S. Blanch, J. Romeu, and I. Corbella, “Exact representation of antenna system diversity performance from input parameter description,” *Electronics Letters*, vol. 39, no. 9, pp. 705–707, May 2003.
- [29] R. Vaughan and J. Andersen, “Antenna diversity in mobile communications,” *IEEE Transactions on Vehicular Technology*, vol. 36, no. 4, pp. 149–172, 1987.
- [30] W. Q. Malik and D. J. Edwards, “Measured mimo capacity and diversity gain with spatial and polar arrays in ultrawideband channels,” *IEEE Transactions on Communications*, vol. 55, no. 12, pp. 2361–2370, Dec 2007.
- [31] H. Shin and J. H. Lee, “Capacity of multiple-antenna fading channels: spatial fading correlation, double scattering, and keyhole,” *IEEE Transactions on Information Theory*, vol. 49, no. 10, pp. 2636–2647, 2003.
- [32] I. Telatar and D. Tse, “Capacity and mutual information of wideband multipath fading channels,” *IEEE Transactions on Information Theory*, vol. 46, no. 4, pp. 1384–1400, 2000.
- [33] J. Jiang, R. Buehrer, and W. Tranter, “Antenna diversity in multiuser data networks,” *IEEE Transactions on Communications*, vol. 52, no. 3, pp. 490–497, 2004.
- [34] M. Simunek, F. P. Fontan, P. Pechac, and F. J. D. Otero, “Space diversity gain in urban area low elevation links for surveillance applications,” *IEEE Transactions on Antennas and Propagation*, vol. 61, no. 12, pp. 6255–6260, 2013.
- [35] A. Paulraj, D. Gore, and R. Nabar, “Performance limits in fading mimo channels,” in *The 5th International Symposium on Wireless Personal Multimedia Communications*, vol. 1, 2002, pp. 7–11 vol.1.
- [36] M. A. Abdalla, D. Z. Nazif, and A. M. Ali, “Two elements Mimo antenna with asymmetric coplanar strip metamaterial configuration and ebg hybrid isolation,” in *2018 12th International Congress on Artificial Materials for Novel Wave Phenomena (Metamaterials)*.
- [37] D. Nazif, I. Mohamed, A. Gaafar, and M. Abdalla, “Uwb notch antennas in mimo system with high isolation performance,” *Radioengineering*, vol. 30, pp. 56–64.
- [38] Y. K. Choukiker, S. K. Sharma, and S. K. Behera, “Hybrid fractal shape planar monopole antenna covering multiband wireless communications with Mimo implementation for handheld mobile devices,” *IEEE Transactions on Antennas and Propagation*, vol. 62, no. 3, pp. 1483–1488.
- [39] D. Sarkar, K. Saurav, and K. V. Srivastava, “A compact four-element csrr-loaded antenna for dual-band pattern diversity mimo applications,” in *2016 46th European Microwave Conference (EuMC)*, 2016, pp. 1315–1318.
- [40] J.-Y. Zhang, F. Zhang, W.-P. Tian, and Y.-L. Luo, “Acs-fed uwb-mimo antenna with shared radiator,” *Electronics letters*, vol. 51, no. 17, pp. 1301–1302, 2015.
- [41] T.-C. Tang and K.-H. Lin, “An ultrawideband mimo antenna with dual band-notched function,” *IEEE Antennas and wireless propagation letters*, vol. 13, pp. 1076–1079.
- [42] Z. Tang, J. Zhan, X. Wu, Z. Xi, L. Chen, and S. Hu, “Design of a compact uwb-mimo antenna with high isolation and dual band-notched characteristics,” *Journal of Electromagnetic Waves and Applications*, vol. 34, no. 4, pp. 500–513.
- [43] L. Kang, H. Li, X. Wang, and X. Shi, “Compact offset microstrip-fed mimo antenna for band-notched uwb applications,” *IEEE Antennas and Wireless Propagation Letters*, vol. 14, pp. 1754–1757.